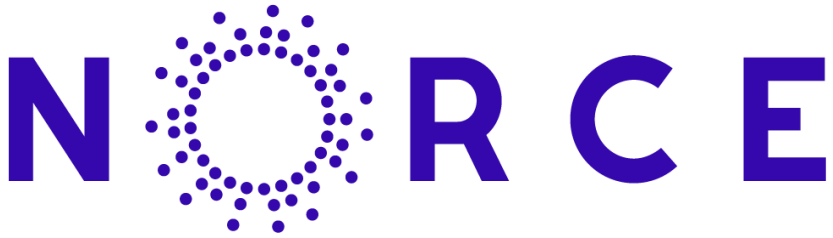

Technical appendix: Theoretic background of snow avalanche detection using Sentinel-1 SAR images

Table of Contents

Characteristics of radar remote sensing

The use of radar satellite data for avalanche detection is advantageous in many ways (Figure 1). Active radar sensors illuminate Earth's surface using microwave radiation and are thus independent of weather or light conditions. The Sentinel-1 satellites deliver free SAR (synthetic aperture radar) data in a consistent manner, enabling near-real time monitoring of medium sized avalanches almost anywhere on Earth (Eckerstorfer et al., 2016).

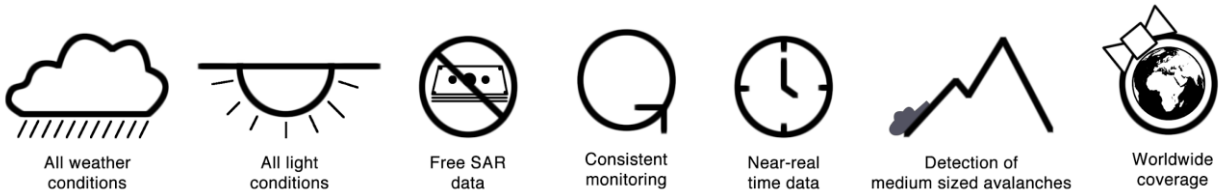

Figure 1: Advantageous characteristics of avalanche detection using Sentinel-1 SAR data.

Sentinel-1 radar satellite constellation and radar sensor parameters

The Sentinel-1 constellation consists of two identical satellites (S1A and S1B) that orbit Earth 180 deg apart. The satellites fly in a sun-synchronous, near-polar orbit with the radar instruments illuminating the surface perpendicular to flight direction (Figure 2). The satellites fly towards and from the North Pole in an ascending and descending orbit respectively.

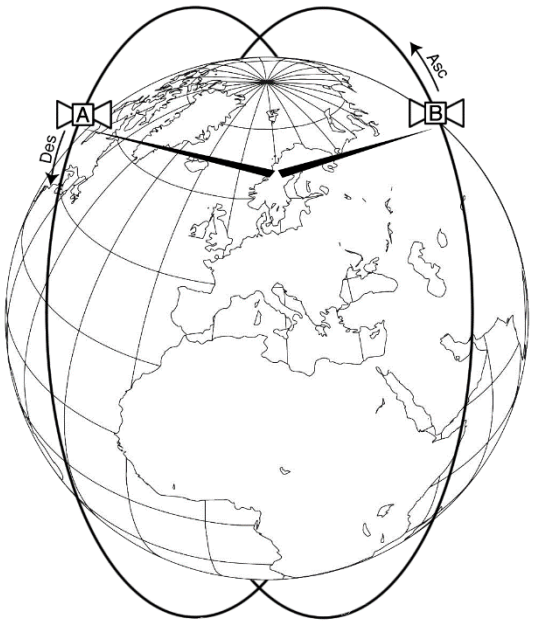

Figure 2: Polar orbits of the Sentinel-1 satellite constellation and the side-looking geometry of the radar sensors.

The radar sensors on board the Sentinel-1 satellites are side-looking instruments with an incidence angle of 29°- 46° with regard to a vertical plane. This leads to radar shadow and layover effects in mountainous terrain (Figure 3).

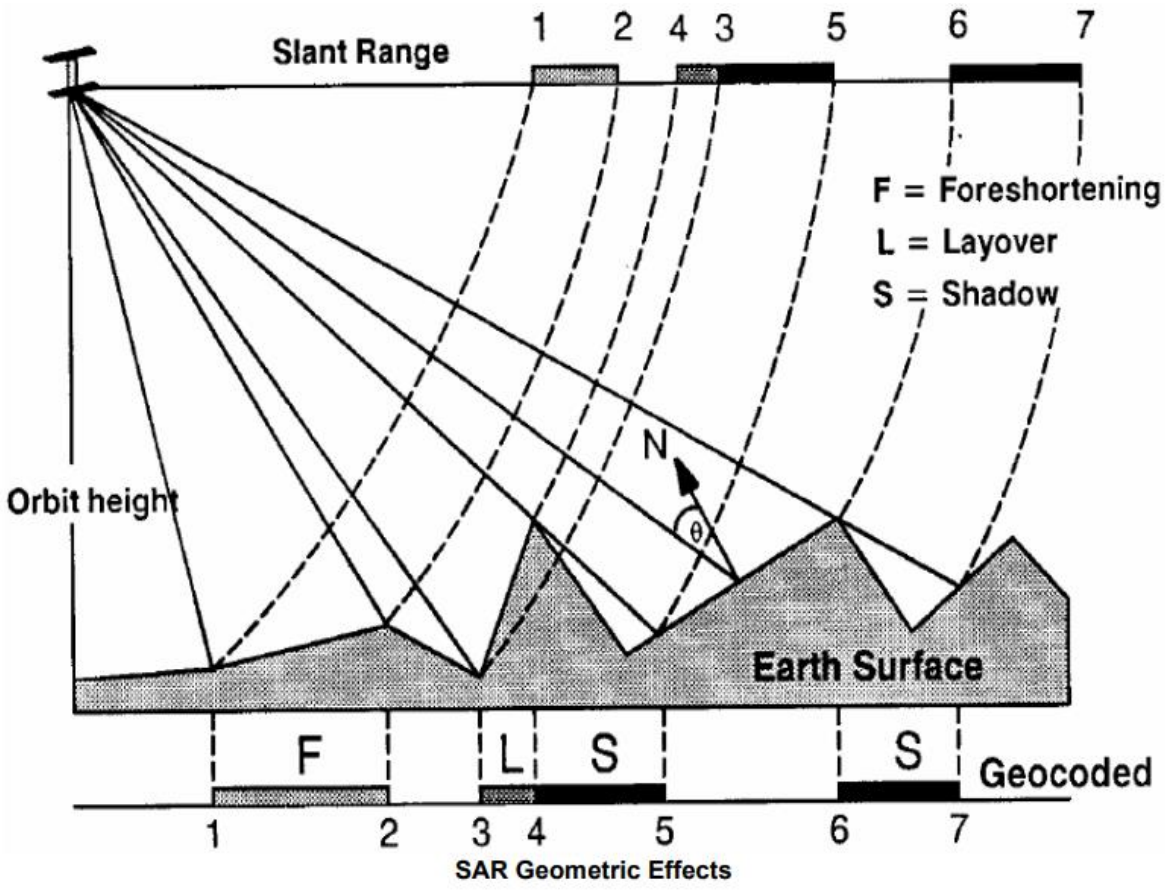

Figure 3: Overview of radar shadow and layover effects induced by the side-looking SAR sensors on board the Sentinel-1 satellites. (from http://step.esa.int/docs/tutorials/S1TBX%20SAR%20Basics%20Tutorial.pdf).

Layover: The top of steep mountains tilted towards the radar sensor and displaced towards the radar from its true position on the ground and therefore "lays over" and distorts the image.

Foreshortening: Happens when the terrain is placed 90° towards the radar sensor.

Shadow: In mountainsides facing away from the radar sensor as the radar cannot "see" through the mountain, thus casting a shadow, where no information can be retrieved.

In Figure 4a we present a single backscatter image from an ascending geometry Sentinel-1 image from 3 April 2017. The whitish, distorted areas are areas effected by radar shadow and layover. Mostly mountain sides facing away from the satellite, towards East, are affected by radar shadows as the Sentinel-1 image was taken while the satellite traveled towards the North Pole, looking down and to the right (East-Northeast). Layover affects steep slopes facing West, towards the satellite. In Figure 4b we masked out all areas affected by radar shadows and layovers.

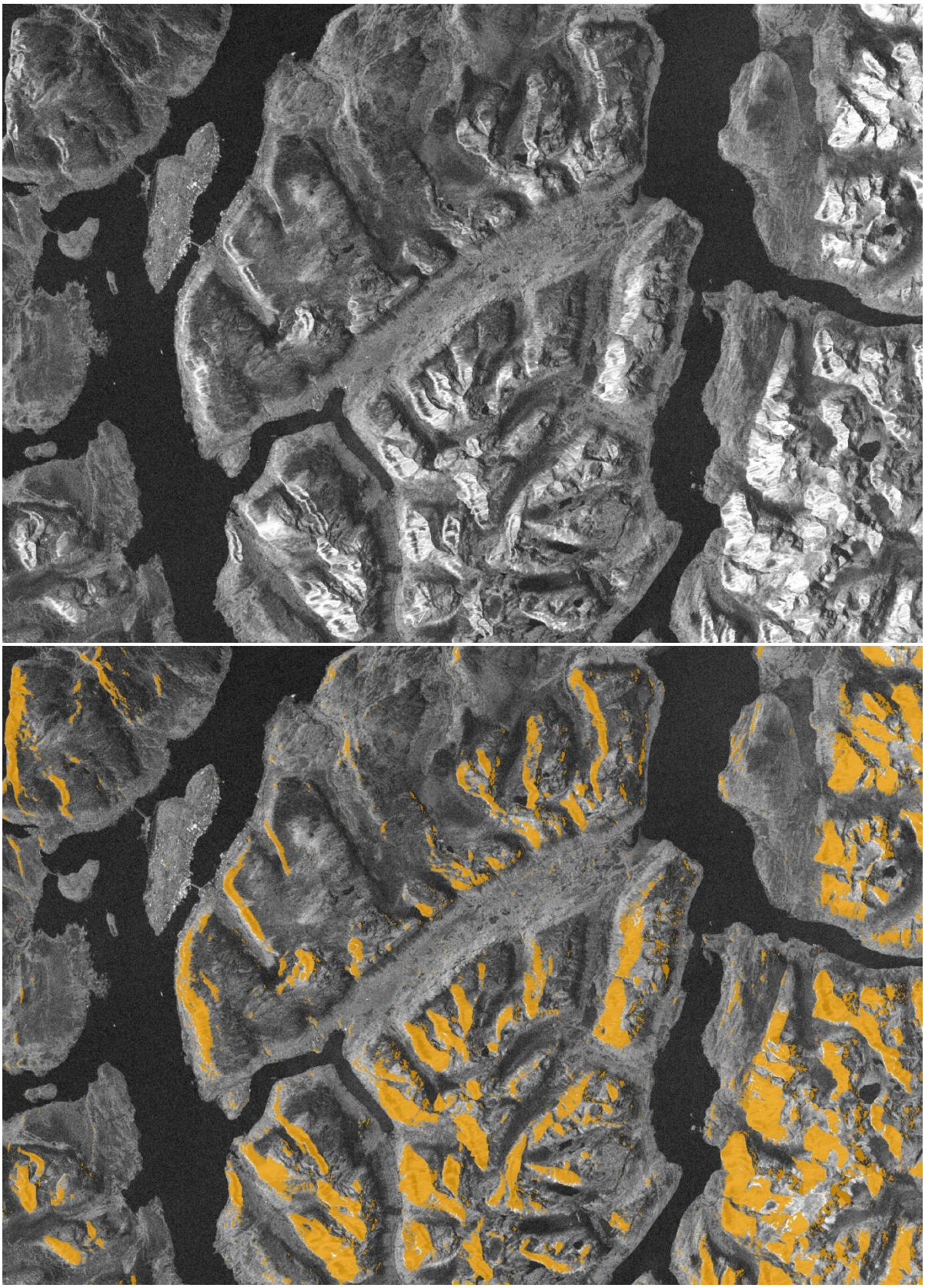

Figure 4: Upper panel: Radar image from 3 April 2017 with radar shadow and layover effected areas visible as distorted, whiteish areas. Lower panel: Same radar image with radar shadow and layover effected areas masked out.

Snow avalanche detection in Sentinel-1 SAR images

Sentinel-1 SAR images can be downloaded from different data hubs. We currently use the Copernicus Collaborative Data Hub (https://colhub.met.no/#/home) to download images as ground range products (GDR). During geocoding of the images, we resample them to a raster resolution of 20 x 20 m. A typical Sentinel-1 image has a ground swath of 250 x 250 km in its interferometric wide swath mode.
Repeat pass time for Sentinel-1 images is 6 days in Norway when considering images of similar geometry and track number. However, due to Norway's high latitude and the polar orbits of the Sentinel-1 satellites, the northern parts of Norway are covered daily, while the southern parts of Norway receive Sentinel-1 images every 2 – 3 days.

Radar backscatter theory from snow and avalanche debris

The radar sensors on board the Sentinel-1 satellites actively emit radar waves in C-band (4-8 GHz frequency) and receive radar backscatter from the ground, with its intensity measured in decibels. Different ground surfaces radiate different amount of energy back.
Snow differs from other surfaces in that the radar signal is highly dynamic. Wet snow has a high water content and absorbs radar waves effectively, giving low measured backscatter and "dark" images. Dry snow differs very little from snowless terrain since the radar waves penetrate the surface and the main signal is returned from the ground under the snow (Figure 5a). The signal strength here is in most cases much stronger than for wet snow.
In case of avalanches, their depositional part, called avalanche debris, constitutes a change in snow depth, snow structure and density, as well as surface roughness, leading to a change in backscatter. This change in backscatter is mainly an increase, relative to the surrounding, undisturbed snowpack, with the majority of backscatter increase stemming from the increased surface roughness (Figure 5b) (Eckerstorfer and Malnes, 2015).

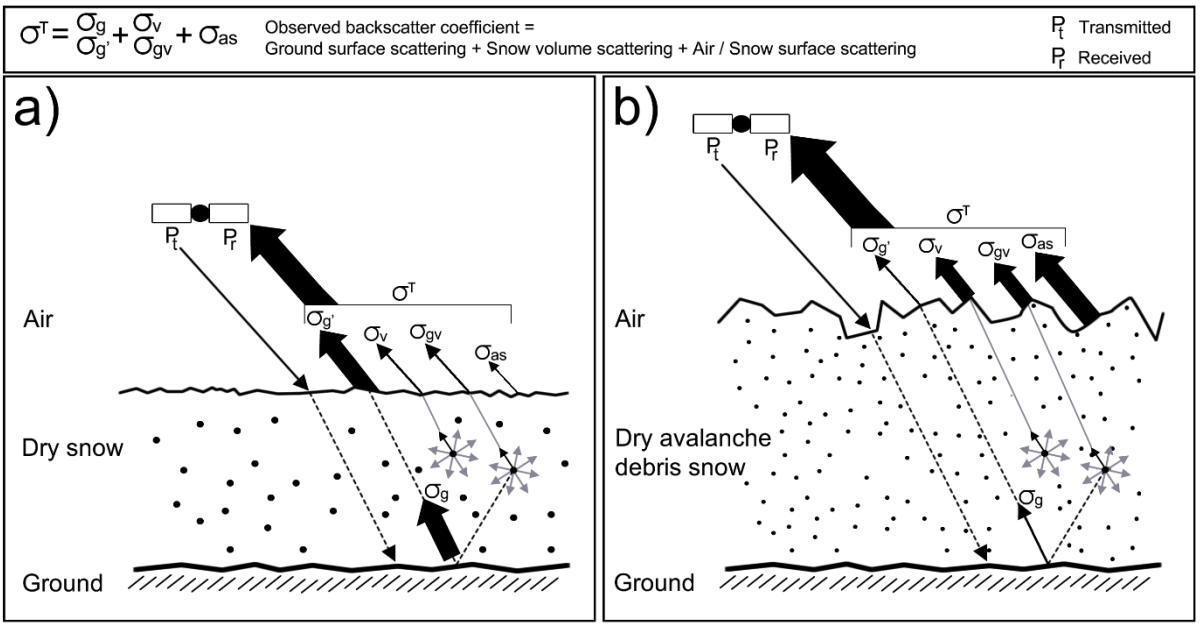

Figure 5: a) Radar backscatter from dry, undisturbed snow, consisting mostly of ground surface scattering. B) Radar backscatter from dry avalanche debris. The increased total backscatter is dominated by the contribution from the rough snow surface. Figure from Eckerstorfer and Malnes (2015).

Temporal change detection of backscatter and manual identification of avalanche debris

To detect avalanche debris, we use a temporal change detection of backscatter. We compare the change in backscatter between two Sentinel-1 images of similar geometry (ASC / DES) and track number,

typically 6 days apart. In Figure 6 we show a reference image from 3 April 2017 (left panel) and an activity image from 9 April 2017 (right panel) when the same image geometry was taken again. Avalanche debris is clearly visible as bright features. Considering only the activity image, one could not tell if the bright features appeared recently or are due to geomorphological features in the landscape that resemble avalanche debris (e.g. debris flow tracks, avalanche talus fans).
We thus combine reference and activity image into a RGB change detection image [R(reference), G(activity), B(reference)] (Figure 7). This way, we color change in backscatter over time, where green resembles backscatter increase in case of fresh avalanche debris, purple depicts backscatter decrease (mainly due to wet snow) and grey areas experienced no backscatter change. In Figure 7 right panel, we show an expert interpretation of avalanche debris visible in the image.

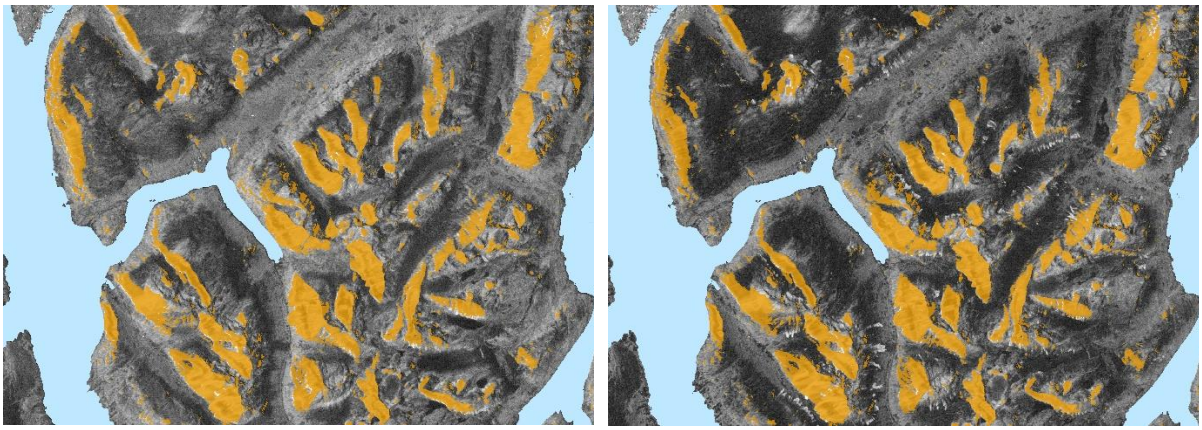

Figure 6: Left panel: Reference image from 3 April 2017 with no visible avalanche activity. Right panel: Activity image from 9 April 2017 with avalanche debris visible as bright features.

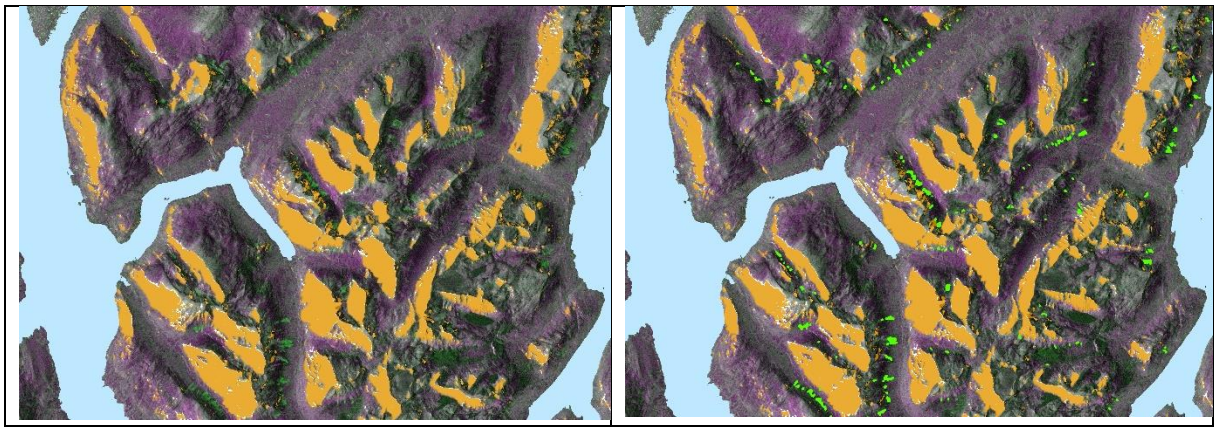

Figure 7: Left panel: RGB change detection image with backscatter change colored (increase = green, decrease = purple, no change = grey). Right panel: Manually identified avalanche debris as polygons in light green. Yellow areas are masked out radar shadow and layover areas.

Expert interpretation of manual detection of RGB change detection images is the golden standard of avalanche detection in Sentinel-1 images. From a dataset of almost 250 field-observed avalanches, we were able to manually detect 77.3 % of them, however 100 % of avalanches with size D3 or larger (length > 1000 m). For avalanches of size D1.5 and 2 (length > 100 m), the probability of detection decreased to 65 and 80 % respectively. However, in general, depending on the distribution of avalanche sizes, roughly 20 % of avalanche activity are not detectable in Sentinel-1 images (Eckerstorfer et al., 2019). The most important reason is avalanche size, however, an unknown number of avalanches may also occur in the radar shadow, exhibit too little increase in relative backscatter change or simply be removed by snow melting or snow blowing before a Sentinel-1 image is taken.

Automatic detection of avalanche debris

We have developed an automatic avalanche detection algorithm that basically also uses temporal change detection of backscatter with several segmentation and classification steps which result in a binary map showing avalanche / non avalanche areas (Vickers et al., 2017, 2016). The binary map is transferred into a vector file, with a polygon outlining each detected avalanche debris and a metadatabase with information on detection time, Sentinel-1 data, location and topographical parameters (Figure 8).

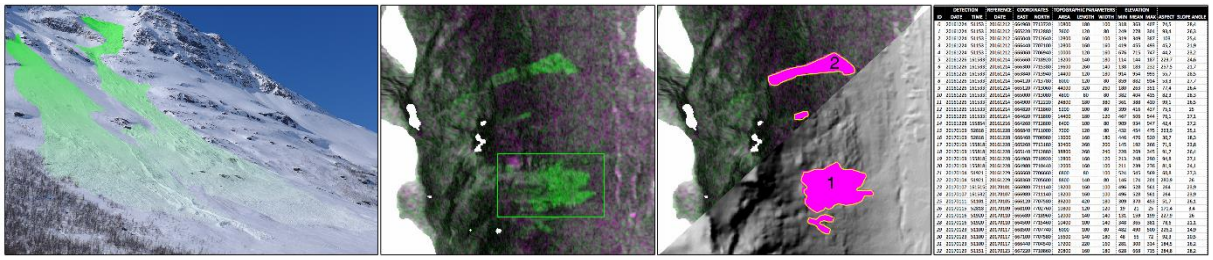

Figure 8: Graphic representation of the workflow from avalanche activity, to change detection images, avalanche detection and associated metadatabase.

Here is the list of parameters that are attached to the avalanche vectors as attribute table:

FID – unique number id
Shape – polygon (similar for all)
OBJECTID – running number
area – area of detected avalanche in square meters
aspect – currently not computed (we are working on it)
det_count – always set at 1
east – x coordinates
length – maximum length of the polygons (not parallel to avalanche path)
north – y coordinates
raster_val – number of detected pixels
refdate – same as T_0
sat_geom – satellite track number
t_0 - reference date (used for constructing change detection images)
t_1 - activity date (date of avalanche detection)
time – same as t_1
track_id – for our use only
uuid – for our use only
width – not computed right now
dem_mean – mean elevation of entire polygon
dem_median – median elevation of entire polygon
dem_min – longest runout (m asl of pixel)
dem_max – furthest upslope position (m asl of pixel)
slp_mean – mean slope angle of entire polygon
slp_min – min slope angle of entire polygon
slp_max – max slope angle of entire polygon
vv1… - backscatter parameters

In order to make automatic detection in large Sentinel-1 images efficient, as well as decrease the number of false alarms, the algorithm detects avalanche debris only in a predefined avalanche runout area. We use the avalanche runout areas defined by NVE for Norway (https://gis3.nve.no/metadata/produktark/Produktark_snoskred_aktsomhet.pdf). This means that

avalanche debris that might stop above or below these runout areas are not detected. We also implemented a minimum cut-off size of 3000 m^2 to further decrease false alarms.

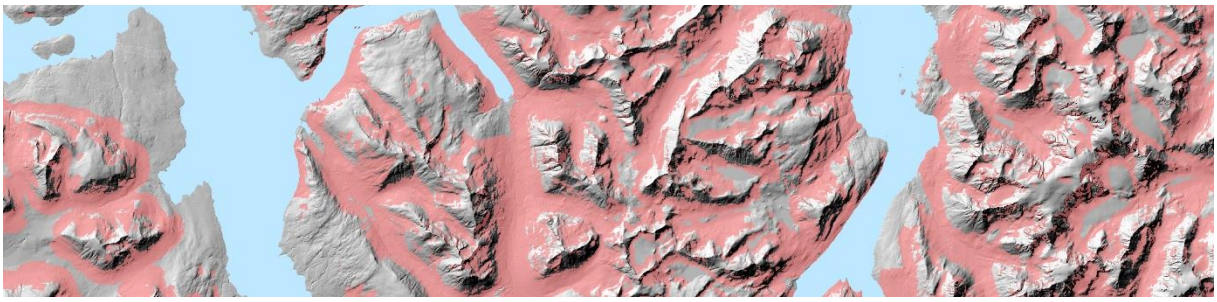

Figure 9: NVE's avalanche runout area in red.

Finally, the algorithm deletes all avalanche debris that is detected more than once (multiple detections) due to up to daily Sentinel-1 images, where the algorithm detects avalanche debris multiple times. In Figure 10 we show a time series of daily avalanche detections, with all detected avalanches shown in green and avalanches without multiple detections shown in pink. The total number of detected avalanches is effectively reduced without any multiple detections biasing the result.

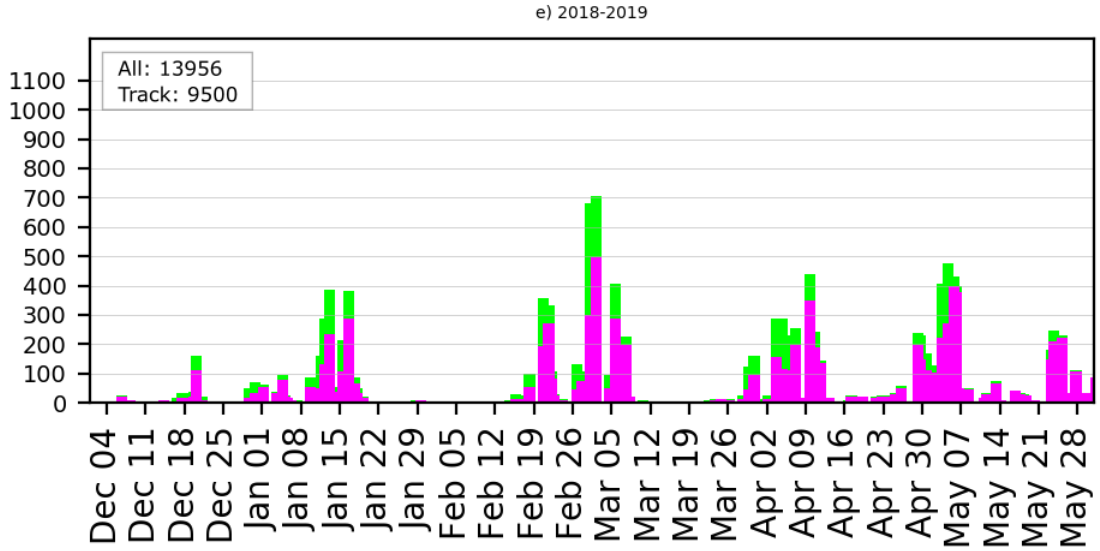

Figure 10: Time series of daily avalanche detections showing all detected avalanches (all: green), and avalanche detections without multiple detections (track: pink). Figure modified from Eckerstorfer et al., (2019).

Possibilities and limitations

Satellite-borne detection of avalanches allows us to monitor large regions for avalanche activity during entire winters. Such a task is not achievable with conventional field-based monitoring. Remote sensing is furthermore economically efficient and timesaving. Nevertheless, remote sensing has its limitations, which cause uncertainties in the interpretation of the data and the deliverables to the end users.

Algorithm performance

Comparing a dataset of field-observed avalanches (N = 250) to automatic avalanche detections yields a probability of detection of 57 %. However, in this dataset of field-observed avalanches, there are

avalanches that are also not manually detectable (due to various reasons explained above). Thus, when considering only manually detectable avalanches from the field dataset, the probability of automatic detection increases to 73 %. Moreover, the detection algorithm is capable of detecting over 90 % of avalanches larger than size D3, while the probability of detection decreases to below 55 % for avalanches of size D1.5 and 2 (Eckerstorfer et al., 2019).

Spatial resolution

As mentioned above, we resample the Sentinel-1 images to 20 m pixel spacing to ensure a high multi-look factor that helps to suppress most SAR speckle artifacts. A spatial resolution of 20 m allows for detection of avalanches with typical path length of 100 m that could bury and kill a person. If large avalanches display thin and elongated shapes, automatic detection might be difficult.

Avalanche delineation

Avalanches are delineated from the contrast in backscatter change between undisturbed snow and avalanche debris. It is mostly the depositional part of an avalanche that is detected due to its high surface roughness. While the lower part of the avalanche debris can be delineated with high confidence (within 20 m pixel spacing), the transition between slide path and avalanche debris displays often a fluid transition. Therefore, avalanche delineation has some degree of uncertainty, which adds uncertainty in calculating avalanche length and area. It is also possible that the algorithm connects detected avalanche debris that lies adjacent to each other or misses parts of an avalanche debris. Nevertheless, comparing our field-observed avalanche activity dataset to automatic detections, 54 % of all avalanches were detected completely, while in 27 % of all cases, adjacent avalanches were connected. Only 17 % of the total were partly detected (Eckerstorfer et al., 2019).

Temporal change detection

A clear backscatter threshold between avalanche debris and undisturbed surrounding snow does not exist. The reason is the dynamic nature of the snowpack, which constantly changes its dielectric properties experienced by the radar wave. Moreover, avalanche debris and surrounding snow are comprised of the same material. In an ideal case, a change detection image displays a transition from dry to wet snow conditions, which results in a relative decrease in backscatter everywhere in the landscape except for avalanche debris which are easily detectable (Figure 11, left panel). Even when the avalanche debris are composed of wet snow, there will be an increase in backscatter due to stronger surface scattering. In the worst-case scenario, the opposite transition from wet to dry snow conditions occurs, which results in an overall increase in backscatter from undisturbed snow (Figure 11, right panel). This makes detection of the avalanche debris challenging due to reduced contrast between undisturbed snow and avalanche debris snow. Both scenarios result in different avalanche detection algorithm performances.

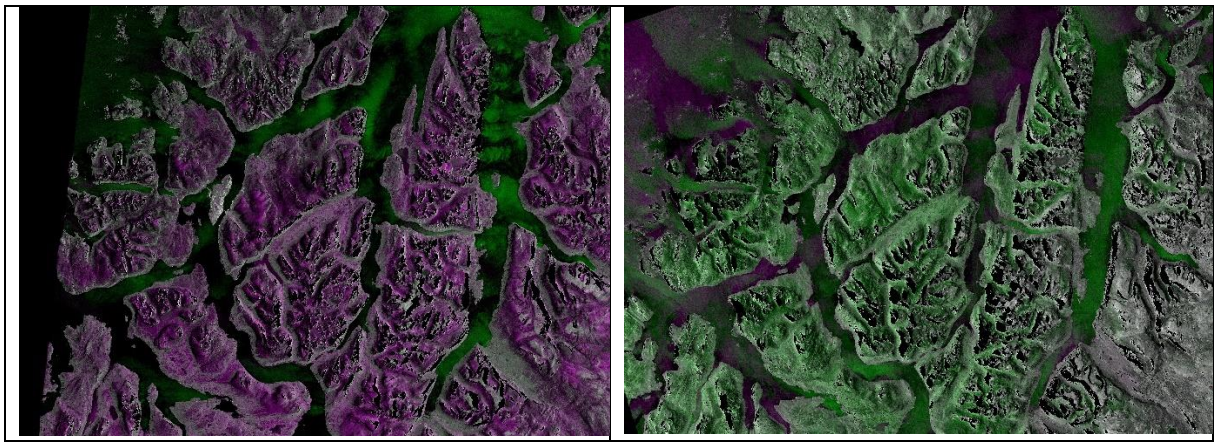

Figure 11: Left panel: Transition from wet to dry snow conditions resulting in a net decrease in backscatter (purple). Right panel: Transition from dry to wet snow conditions resulting in a net increase in backscatter (green). Radar shadow and layover areas are black.

References

Eckerstorfer, M., Bühler, Y., Frauenfelder, R., Malnes, E., 2016. Remote sensing of snow avalanches: recent advances, potential, and limitations. Cold Regions Science and Technology 121, 126–140. https://doi.org/10.1016/j.coldregions.2015.11.001

Eckerstorfer, M., Malnes, E., 2015. Manual detection of snow avalanche debris using high-resolution Radarsat-2 SAR images. Cold Regions Science and Technology 120, 205–218. https://doi.org/10.1016/j.coldregions.2015.08.016

Eckerstorfer, M., Vickers, H., Malnes, E., Grahn, J., 2019. Near-Real Time Automatic Snow Avalanche Activity Monitoring System Using Sentinel-1 SAR Data in Norway. Remote Sensing 11, 2863. https://doi.org/10.3390/rs11232863

Vickers, H., Eckerstorfer, M., Malnes, E., Doulgeris, A., 2017. Synthetic Aperture Radar (SAR) Monitoring of Avalanche Activity: An Automated Detection Scheme, in: Sharma, P., Bianchi, F.M. (Eds.), Image Analysis. Springer International Publishing, Cham, pp. 136–146. https://doi.org/10.1007/978-3-319-59129-2_12

Vickers, H., Eckerstorfer, M., Malnes, E., Larsen, Y., Hindberg, H., 2016. A method for automated snow avalanche debris detection through use of synthetic aperture radar (SAR) imaging. Earth and Space Science 18. https://doi.org/10.1002/2016E000168